

Review Article



A Modified Echocardiographic Classification of Mitral Valve Regurgitation Mechanism: The Role of Three-dimensional Echocardiography

Lotte E. de Groot-de Laat , MD^{1,2}, Jackie McGhie , MSc, PhD¹, Ben Ren , MD, PhD¹, René Frowijn , MSc¹, Frans B. Oei , MD, PhD², and Marcel L. Geleijnse , MD, PhD¹

¹Department of Cardiology, Thoraxcenter, Erasmus University Medical Center, Rotterdam, the Netherlands

²Department of Cardiothoracic Surgery, Thoraxcenter, Erasmus University Medical Center, Rotterdam, the Netherlands



Received: Jan 25, 2019

Revised: Mar 27, 2019

Accepted: Apr 8, 2019

Address for Correspondence:

Lotte E. de Groot-de Laat, MD

Departments of Cardiology and Cardiothoracic Surgery, Erasmus University Medical Center, Thoraxcenter, Room RG 427, Doctor Molewaterplein 40, 3015 GD Rotterdam, the Netherlands.
E-mail: l.delaat@erasmusmc.nl

Copyright © 2019 Korean Society of Echocardiography

This is an Open Access article distributed under the terms of the Creative Commons Attribution Non-Commercial License (<https://creativecommons.org/licenses/by-nc/4.0/>) which permits unrestricted non-commercial use, distribution, and reproduction in any medium, provided the original work is properly cited.

ORCID iDs

Lotte E. de Groot-de Laat
<https://orcid.org/0000-0001-9821-9569>
Jackie McGhie
<https://orcid.org/0000-0001-6359-4115>
Ben Ren
<https://orcid.org/0000-0002-8227-8094>
René Frowijn
<https://orcid.org/0000-0002-6214-008X>
Frans B. Oei
<https://orcid.org/0000-0003-2412-0026>
Marcel L. Geleijnse
<https://orcid.org/0000-0002-0941-3384>

ABSTRACT

In this report, we provide an overview of a new, updated echocardiographic classification of mitral regurgitation mechanisms to provide a more comprehensive and detailed assessment of mitral valve disorders. This is relevant to modern mitral valve repair techniques, with special attention to the added value of 3D-echocardiography.

Keywords: Mitral regurgitation; Mechanism; Echocardiography; Three-dimensional echocardiography

INTRODUCTION

Pre-operative echocardiographic assessment of MV pathology has become of crucial importance with the transition from prosthetic mitral valve (MV) replacement to MV repair in the last decades. This has more recently been facilitated by development of newer echocardiographic techniques such as three-dimensional (3D) imaging^(1,2) and simultaneous biplane imaging.^(3,4)

Communication between the cardiologist and the surgeon is as important as the obtained echocardiographic information. Therefore, in 1983, Carpentier⁽⁵⁾ proposed a clearly defined, universal MV leaflet terminology. The normal MV is comprised of an anterior leaflet connected on either side through the anterolateral and posteromedial commissures to the posterior leaflet. The anterior leaflet occupies two-thirds of the valve area, whereas the posterior leaflet occupies only one-third, and the latter leaflet is connected to two-thirds of the annulus. The posterior leaflet consists of three scallops or segments: the lateral scallop is labeled P1, the middle scallop P2, and the medial scallop P3. Although the anterior leaflet is smooth without natural scallops, the leaflet parts opposing the corresponding posterior leaflet scallops are accordingly labeled A1, A2, and A3. Because the P2 scallop is relatively large, it may be divided into lateral and medial halves (P2L and P2M) or even divided into three parts: centro-lateral (P2CL), central (P2C), and centro-medial (P2CM). The two commissures are usually also composed of small scallops and may be designated as the lateral commissural scallop (CL) and medial commissural scallop (CM).⁽⁶⁾ The chordae arising from the anterolateral

Conflict of Interest

The authors have no financial conflicts of interest.

Table 1. Echocardiography-based classification of mitral valve pathology

Type I: Normal leaflet motion
A. Leaflet perforation
B. Congenital cleft
C. Dilated annulus (without leaflet tethering)
Type II: Increased leaflet motion
A. Localized prolapse or flail scallop
B. Billowing leaflets with prolapse
C. Billowing leaflets with a flail segment
Type III: Restricted leaflet motion
A. Systolic and diastolic restriction
B. Symmetric systolic restriction
C. Asymmetric systolic restriction
Type IV: Systolic anterior motion
A. Hypertrophic cardiomyopathy
B. Post-mitral valve repair
C. Hemodynamically-induced (hypovolemia, inotropic stimulation)
Type V: Hybrid conditions
Examples
- Prolapse of a leaflet combined with systolic anterior motion or a restricted leaflet
- Intrinsic pathology with superimposed infective endocarditis lesion

Modified from Shah and Raney⁷⁽⁸⁾

papillary muscle are attached to CL, A1, P1, A2L, and P2L, whereas those arising from the posteromedial papillary muscle are attached to CM, A3, P3, A2M, and P2M.

In addition to the leaflets and their scallops, the MV apparatus includes an annulus, chordae tendineae, papillary muscles, and the left ventricle (LV). Mitral regurgitation (MR) may develop when any part of the MV apparatus becomes abnormal. Carpentier⁵⁾ described the pathophysiologic classification of the three types of MV pathology on the basis of a functional approach that were linked to specific repair techniques. Type I involves normal leaflet motion, type II is associated with increased leaflet motion, and type III is associated with restricted leaflet motion.

More recently, Shah and Raney⁷⁽⁸⁾ proposed a modified echocardiographic classification of MR mechanisms to provide a more comprehensive and detailed assessment of MV disorders that is relevant to modern MV repair techniques. In this report, we give an overview of the Shah and Raney pathological MR classification (**Table 1**), with special attention to the added value of 3D-echocardiography. The focus is on trans-esophageal 3D imaging because, in our experience, 3D transthoracic imaging of the MV has limited accuracy even in the hands of experts.³⁽⁹⁾⁽¹¹⁾

CLASSIFICATION OF MV PATHOLOGY

Type I: Normal leaflet motion

This type of pathology is the same as in the original Carpentier classification. The MV leaflets have normal excursion and subannular leaflet coaptation without a tenting or tethering appearance. Underlying pathologies for MR of this type are now sub-categorized as leaflet perforation (Type I-A), congenital cleft deformity (Type I-B), and pure annular dilatation without leaflet tethering (Type I-C).

MV leaflet perforation can be the result of trauma but is most commonly caused by localized infective tissue destruction. Other than primary MV endocarditis, aortic valve endocarditis

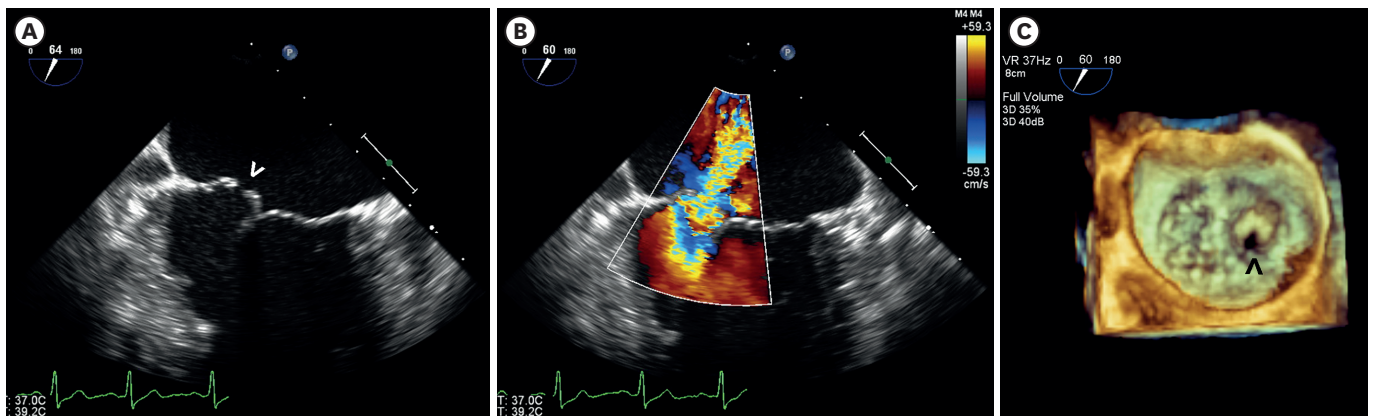


Figure 1. Mitral valve perforation in the medial part of the anterior leaflet, identified with 2D grayscale (A, see arrowhead), 2D color (B), and with 3D echo from the left atrial (surgical) view (C, see arrowhead).

can also directly extend toward the anterior MV leaflet via the anatomically shared fibrous trigones or be transmitted via the aortic valve regurgitation blood jet.¹²⁾ Three-dimensional echocardiography provides added benefit to traditional two-dimensional (2D) imaging because of its ability to provide en-face visualization of the MV, allowing more precise anatomical localization and measurement of the size of the leaflet perforation, as seen in **Figure 1**.¹³⁾

A congenital cleft of the MV is most commonly seen in association with an atrioventricular canal defect, but an isolated cleft of the anterior or posterior MV leaflet has also been described.¹⁴⁾ In this subtype, 3D echocardiography provides superior diagnostic accuracy and may improve surgical results.¹⁵⁾¹⁶⁾ An MV cleft can be easily seen on the 3D image from both the atrial (**Figure 2A**) and ventricular (**Figure 2B**) aspects of the MV, whereas it is often extremely challenging to make the correct diagnosis with 2D echocardiography. It is important to differentiate true clefts from drop-outs (facilitated by use of color Doppler) and pseudo clefts from deep folds in myxomatous MV disease, particularly post-MV repair.

Mitral annulus dilatation is usually seen in combination with the later described types II and III MR.¹⁷⁾ Pure or isolated mitral annulus dilatation in the absence of leaflet tethering or

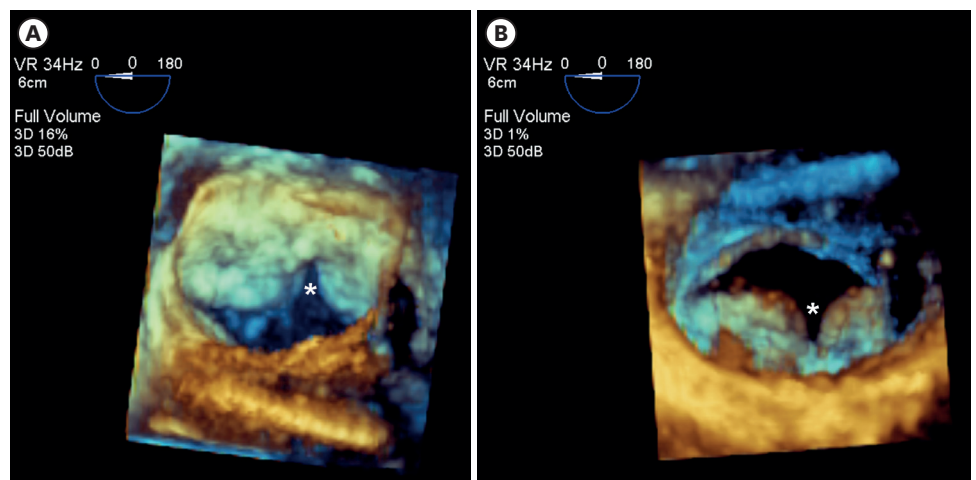


Figure 2. Three-dimensional echocardiographic surgical view of an anterior mitral valve leaflet cleft seen from the left atrial (surgical) view (A, see asterisk) and left ventricular view (B, see asterisk).

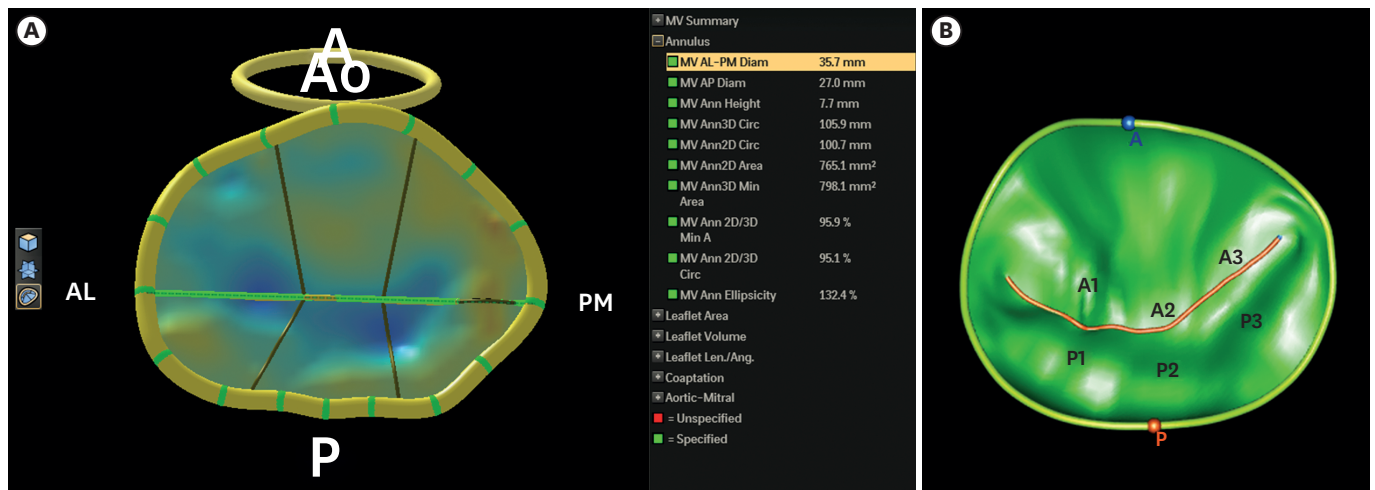


Figure 3. Three-dimensional echocardiographic surgical view reconstruction of the mitral annulus with software from Philips QLAB (A) and TomTec (B).

prolapse is mainly seen in patients with chronic atrial fibrillation but also in patients with heart failure with preserved LV function.¹⁸⁾ The location of MV leaflet coaptation with respect to the annulus is normal, but the zone or surface of coaptation is reduced, resulting in central MR. The definition of annulus dilatation with 2D echocardiography is limited by lack of clear data regarding the best echocardiographic view in which it should be measured.¹⁹⁾²⁰⁾ The apical 4-chamber view is recommended in some instances,²¹⁾ although it is well known that this view does not represent a consistent or reproducible axis of the mitral annulus.²²⁾⁻²⁴⁾ In contrast, 3D echocardiography provides an en-face view of the mitral annulus from which multi-planar reconstruction or modeling of the MV enables precise measurements not only of the major and minor axes, but also of the complete annular circumference (**Figure 3**).

Type II: Increased leaflet motion

This type is characterized by MV leaflets exhibiting excess excursion into the left atrium and is also the same as in the original Carpentier classification but now has three subtypes. In type II-A there is typically fibro-elastic deficiency with thin and friable chordae that lead to a prolapsing segment due to chordal elongation, eventually resulting in a flail leaflet prolapse due to chordal rupture (**Figure 4A**). Acute flail leaflet prolapse may also be the result of chordal rupture in acute endocarditis or (less often) papillary muscle rupture due to acute myocardial infarction (**Figures 4B to 4E**). The MR jet in this type is always eccentric: anteriorly directed in posterior MV leaflet prolapse and posteriorly directed in anterior MV leaflet prolapse. A late-systolic central jet may be seen in billowing leaflets due to chordal elongation (Type II-B, **Figures 5A to 5C**). In its extreme form, there is significantly increased diffuse redundant and thickened leaflet tissue due to myxoid infiltration and annulus dilatation with multiplecental and eccentric regurgitant jets known as myxomatous Barlow's disease (**Figures 5D and 5E**). In patients with more severe chordal elongation, the regurgitant jets may occur earlier in systole. The combination of these two types results in a third subtype consisting of billowing leaflets with associated flail due to chordal rupture that also results in multiple jets (Type II-C).

Of note, the terms flail, prolapse, and billowing MV are often used differently, especially between cardiologists and surgeons. Billowing refers to passing of only the body of the MV leaflet above the mitral annular plane (**Figures 5A to 5C**), whereas prolapse means that the

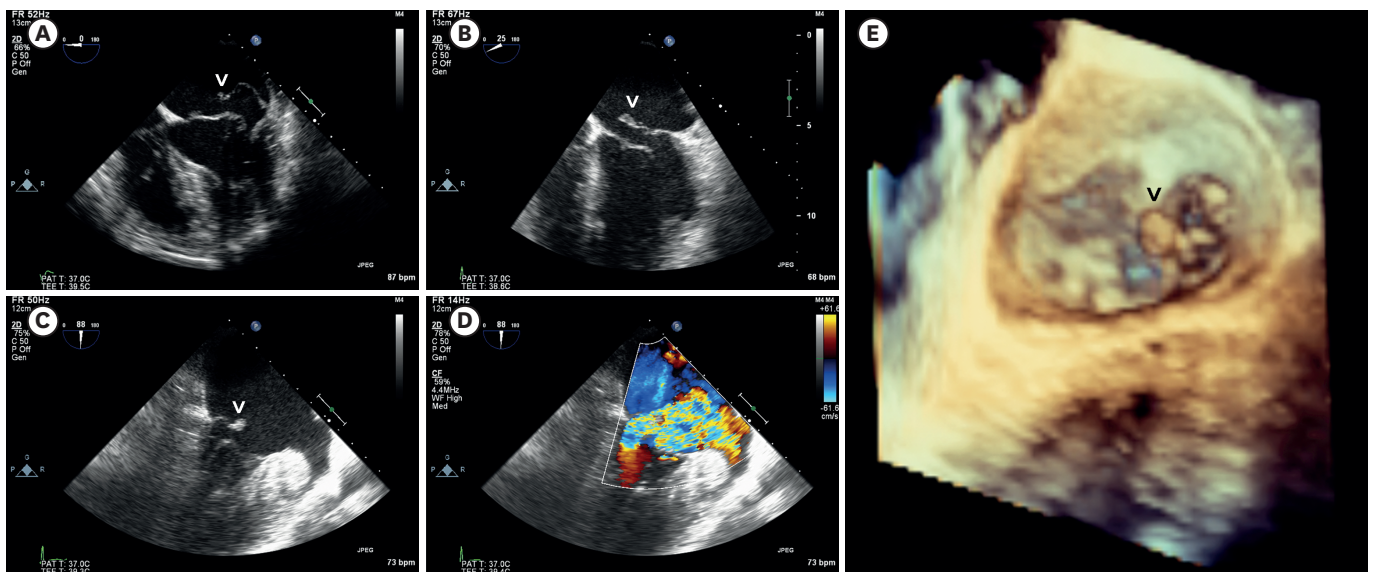


Figure 4. Type II-A mitral valve prolapse due to fibro-elastic deficiency with chordal rupture (A, see arrowhead). Acute flail mitral valve leaflet prolapse due to antero-lateral papillary muscle rupture (B, see arrowhead) and postero-medial papillary muscle rupture (C: gray-scale, see arrowhead, D: color Doppler, E: 3D image, see arrowhead).

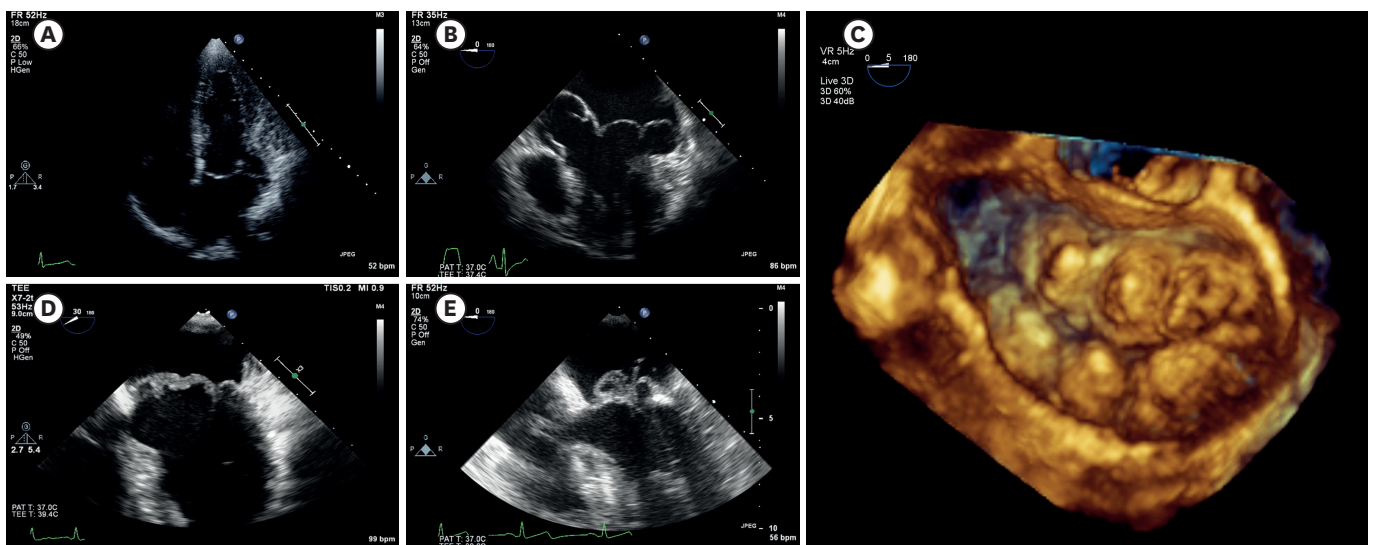


Figure 5. Type II-B billowing mitral valve leaflets due to chordal elongation seen with 2D transthoracic (A), 2D trans-esophageal (B), and 3D echocardiography (C: surgical view). Diffuse redundant and thickened leaflet tissue known as myxomatous Barlow's disease is seen with trans-esophageal echocardiography without (D: type II-B) and with chordal ruptures (E: type II-C).

leaflet tips are also above the mitral annular plane. Prolapse, unlike billowing, is always associated with MR. A flail MV leaflet is an extreme form of prolapse associated with chordal rupture (**Figure 4A**) or extreme chordal elongation without rupture.

The presence, location, and extent of prolapse are of crucial importance in defining the likelihood of successful MV repair.²⁵⁾²⁶⁾ Compared to 2D imaging, 3D echocardiography obviates the need to mentally reconstruct the MV in three dimensions from multiple 2D images to understand the underlying MV anatomy. The entire MV can be visualized in a single image, making it possible to examine both leaflets from the left atrial (surgical) perspective,

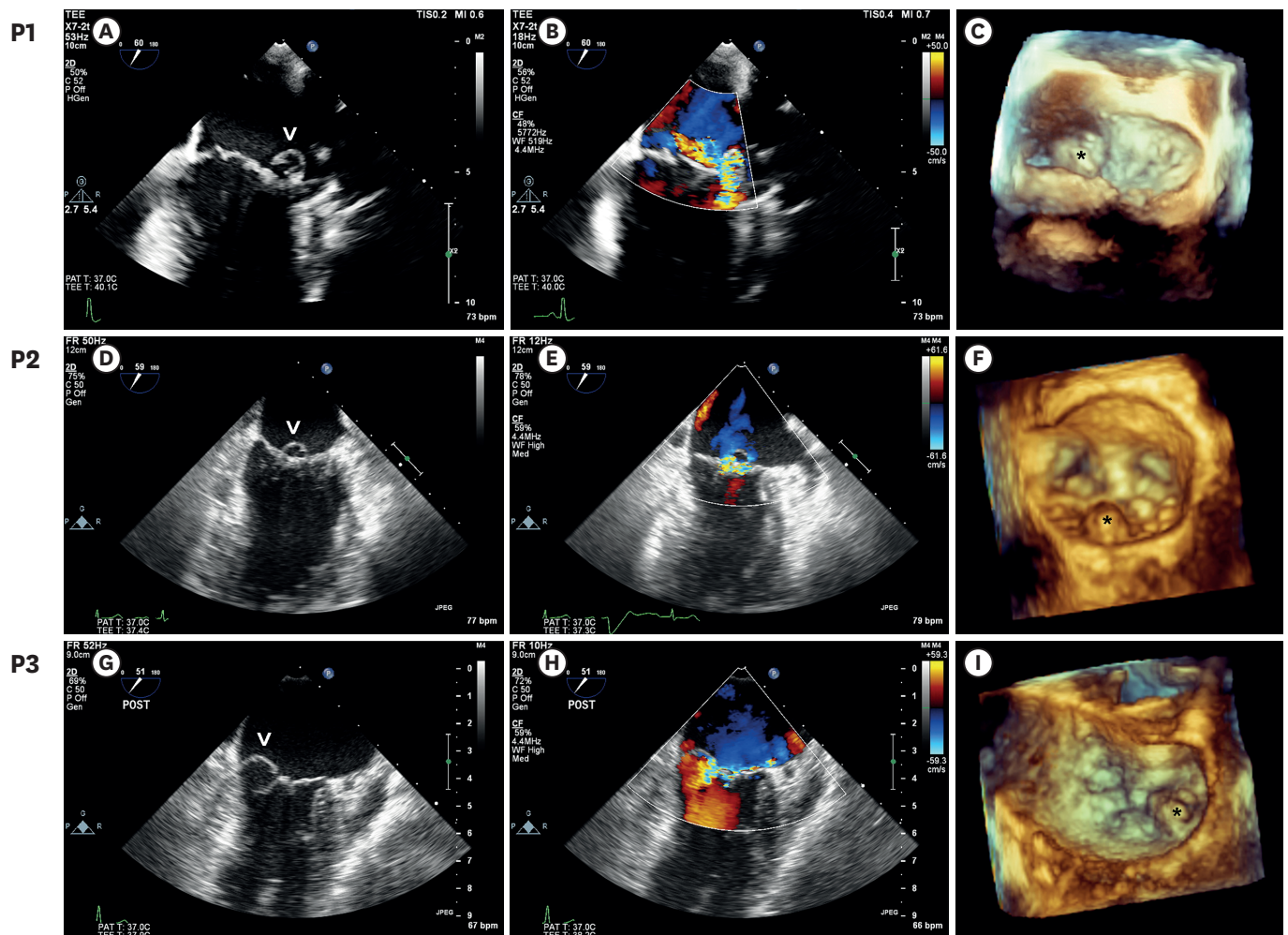


Figure 6. Mitral valve prolapse site identification with trans-esophageal commissural view 2D imaging (left column), color-imaging (middle column), and 3D imaging (right column). Seen are prolapses (asterisks and arrowheads) of the P1 (top row A-C), P2 (middle row D-F), and P3 (bottom row G-I) scallops.

which allows more definitive identification of the localization (**Figure 6**) and extent (**Figure 7**) of prolapse. This technique may also be less operator dependent because it does not require the finesse of probe manipulation to delineate MV pathology. Several studies have shown that time to diagnosis was considerably faster and diagnostic accuracy improved with 3D echocardiography, in particular for identification of P1 and P3 prolapse.⁶⁾

Type III: Restricted MV leaflet motion

In the original Carpentier classification, type III was divided into two subtypes: IIIA with restricted opening and IIIB with restricted closure. Shah and Raney⁸⁾ proposed division of this type into three subtypes.⁵⁾

Type III-A is characterized by systolic and diastolic restriction as seen in rheumatic and other inflammatory pathologies and is associated with commissural fusion, chordal shortening, and fibrosis. The leaflets are thickened and shortened, resulting in inadequate coaptation and regurgitation (**Figures 8A** and **8B**). The main role for 3D echocardiography in this subtype is assessment of the MV area, and this has become the reference method of classifying MV stenosis (**Figure 8C**)²⁷⁾²⁸⁾ because it facilitates imaging of the true narrowest opening of the

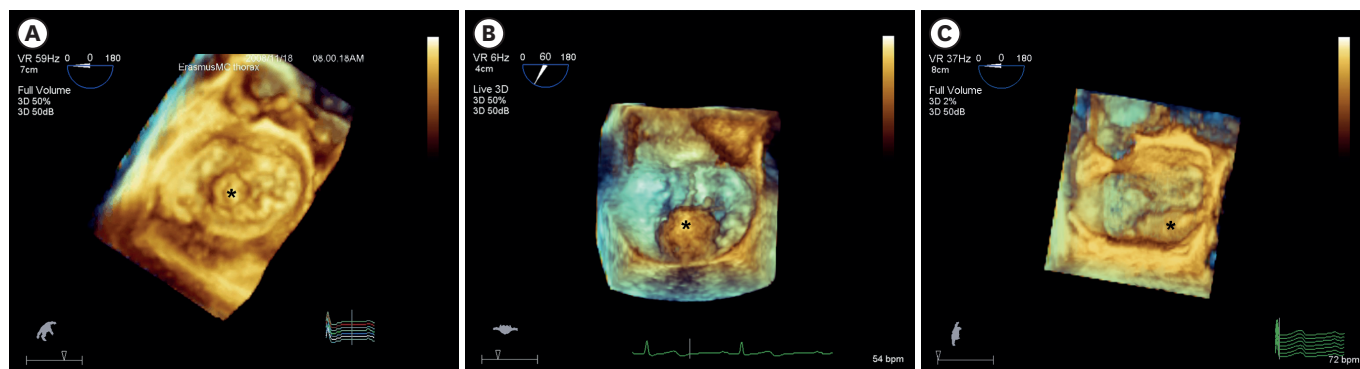


Figure 7. Three-dimensional echocardiographic surgical view of mitral prolapse extent: small P2 prolapse (A), broad P2 prolapse (B), and P2-P3 prolapse (C). The sites of prolapse are indicated with arrowheads.

MV orifice. Still, it should be recognized that this measurement is – as the 2D measurement – challenging in the presence of severe calcification. The use of a 3D Wilkins score may improve the traditional 2D Wilkins score for selection of patients suitable for MV plasty.²⁹⁾³⁰⁾

In types III-B and III-C, there is systolic restriction with one or more tethered leaflets. Tethering on echocardiography is characterized by systolic displacement of one or more leaflets from the annular plane.³¹⁾³²⁾ The closure and position of mitral leaflets are determined by the balance between two forces acting on them: the closing forces generated by the LV systolic contraction, which effectively closes the valve, and the tethering forces, which restrain the leaflets to prevent leaflet prolapse. When tethering is increased by outward displacement of the papillary muscles and the closure forces are reduced by LV dysfunction, the equilibrium between these two forces is disrupted in favor of tethering forces, with displacement of the coaptation point of the leaflets in the ventricle.

Two tethering patterns have been described³³⁾ and in the new approach are classified as type III-B symmetric (**Figures 8D and 8E**) and type III-C asymmetric (**Figures 8F and 8G**) restriction. Systolic symmetric tethering with central MR is seen in dilated or chronic global ischemic cardiomyopathy with outward displacement of the papillary muscles and annulus dilatation with the point of coaptation remaining at the leaflet tips but displaced toward the apex with a reduction in coaptation zone.³³⁾ The severity of this type of MR is greatly related to dynamic changes in loading conditions seen in treatment with diuretics, afterload reducing agents, or general anesthesia (**Figure 9**).³⁴⁾ 3D echocardiography may quantify dynamic changes that occur in the mitral annular surface and its 3D longitudinal displacement and characterize the complex geometric relationship between the papillary muscles and the MV apparatus.³⁵⁾ Some have advocated measurement of the tenting pattern, especially regional 3D tethering of segment P3, as a predictor of long-term prognosis in patients with dilated cardiomyopathy³⁶⁾ or as a predictor of recurrent ischemic MR after undersized mitral ring annuloplasty.³⁷⁾

Asymmetric systolic restriction as seen in type III-C (**Figures 8F and 8G**) typically occurs in patients with a localized posterior wall motion abnormality and results in tethering of the corresponding leaflet, whereas the other normal leaflet overrides the point of coaptation without going above the annular plane. It is important to recognize that this latter leaflet is thus not prolapsing but only overriding a restricted opposite leaflet.

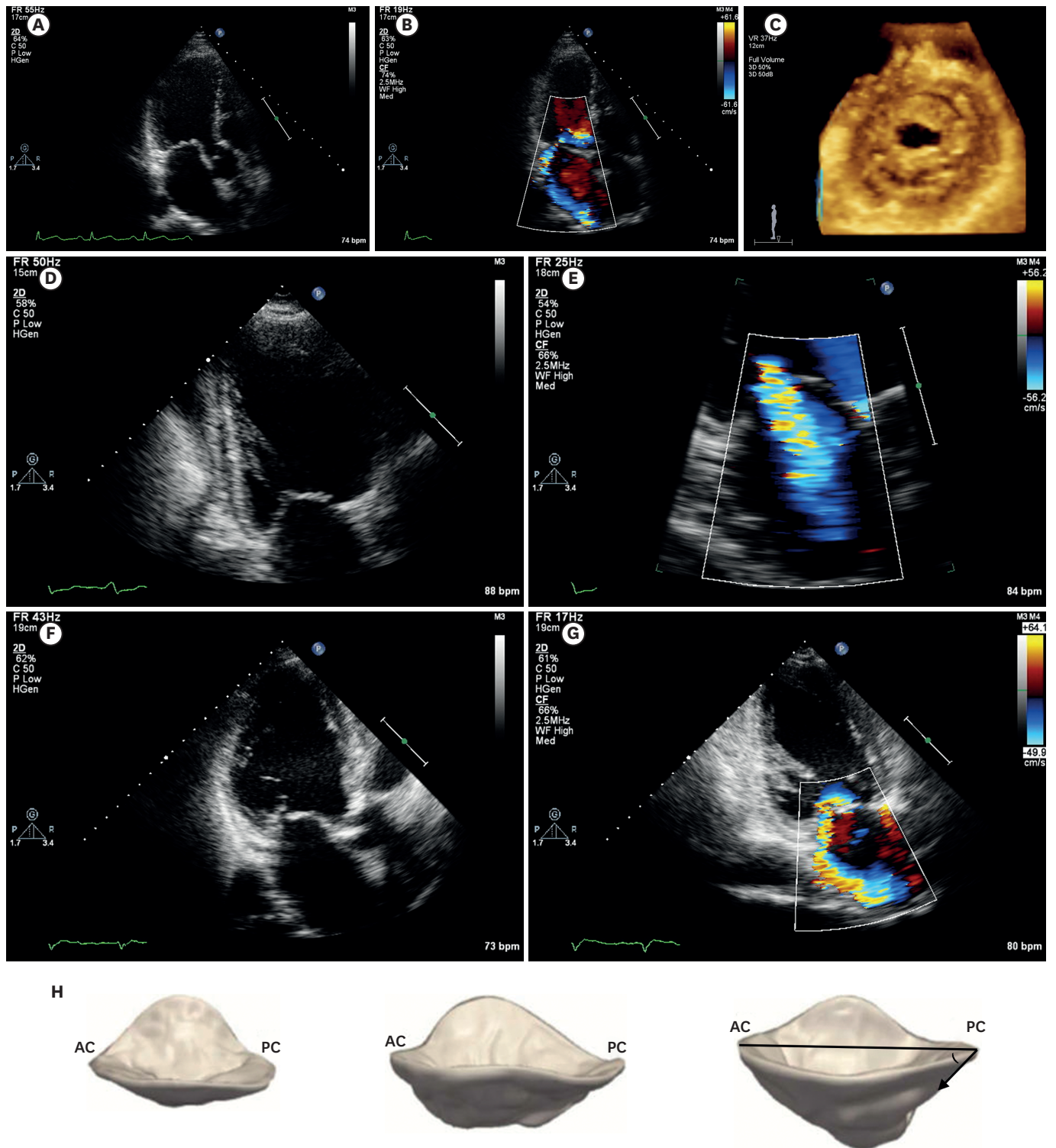


Figure 8. Mitral valve restriction seen with 2D trans-thoracic gray scale and color imaging in rheumatic disease with systolic and diastolic restriction (A, B, and C) and the 3D surgical view with reduced valve opening) in dilated cardiomyopathy with symmetric systolic restriction (D and E) and ischemic cardiomyopathy (F and G) with asymmetric systolic restriction. In the bottom panel (H), 3D echocardiographic virtual models are seen from the commissure-to-commissure view. The 3D tenting area and tethering angle of segment P3 (arrow-line) may predict recurrent mitral regurgitation after annuloplasty. AC denotes anterior commissure and PC denotes posterior commissure. Reproduced with permission from Bouma et al.³⁷⁾

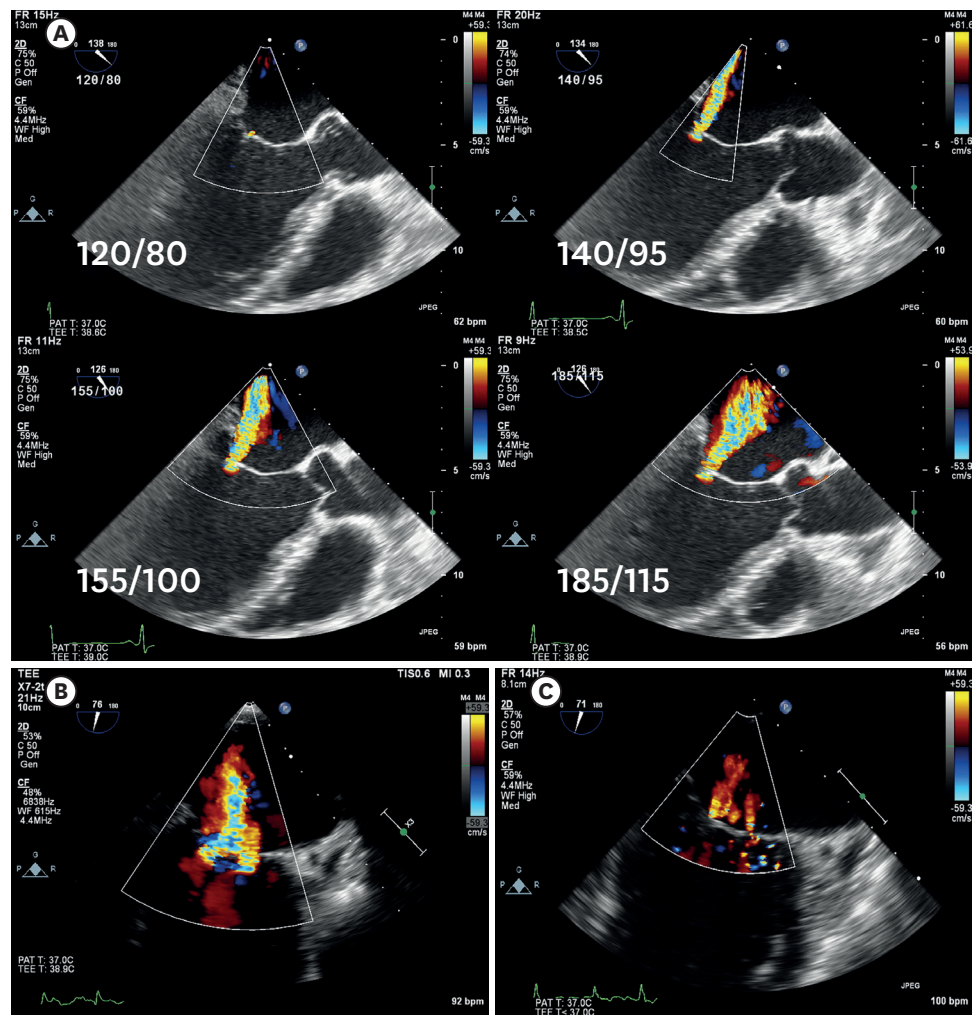


Figure 9. Influence on the severity of trans-esophageal assessment of mitral regurgitation by peri-operative blood pressure changes (A) and general anesthesia (B: significant mitral regurgitation in the outpatient clinic, C: minimal mitral regurgitation under general anesthesia).

Type IV: Systolic anterior motion

Systolic anterior motion (SAM) of the MV may lead to significant MR and is seen in different circumstances. In general, the role of 3D echocardiography in recognition of SAM is minimal.

Type IV-A is seen in hypertrophic cardiomyopathy characterized by anteriorly displaced papillary muscles and elongated MV leaflets with a residual portion of the anterior MV leaflet extending beyond the point of coaptation.³⁸⁾ This portion is not constrained by the left atrial – ventricular pressure differences but freely moves with the flow in the LV outflow tract. In particular, in patients with a relatively short posterior MV leaflet, SAM causes an eccentric MR jet directed laterally and posteriorly (**Figure 10A**).

Type IV-B is seen after MV repair. Pathologic motion of the distal MV leaflet as described above may be simulated by a disproportionate reduction of the MV annulus compared to the size of post-repair MV leaflet tissue (**Figures 10B and 10C**).

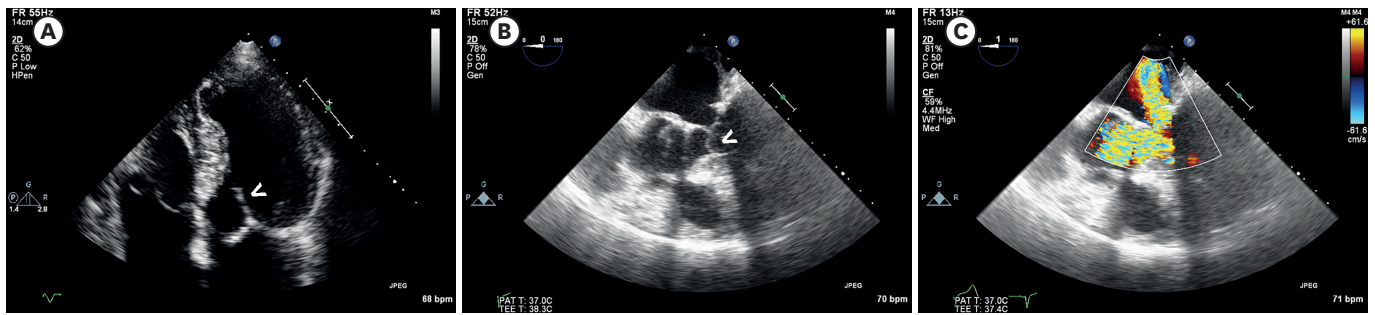


Figure 10. Mitral regurgitation due to systolic anterior motion (see arrowheads) in hypertrophic cardiomyopathy (A) and after mitral valve annuloplasty (B: gray-scale and C: color Doppler).

Type IV-C is seen in a hypovolemic, hyperdynamic LV. Typically it is seen during dobutamine stress³⁹⁾ or with excess doses of inotropics in hypotensive states, paradoxically worsening hypotension.

Type V: Hybrid motion in co-existing pathologies

Hybrid pathologies include combinations of more than one pathology in a patient. Examples include intrinsic pathology with a superimposed infective endocarditis lesion and restrictive posterior leaflet pathology combined with anterior leaflet prolapse or SAM.

SPECIFIC ROLES OF 3D COLOR IMAGING IN ASSESSMENT OF MV PATHOLOGY

The main application of 3D color imaging for assessment of MV pathology is in assessment of paravalvular leakage after MV surgery.⁴⁰⁾ Evaluation of the extent and shape of the leaking orifice and the site of annulus detachment is critical in assessment of paravalvular leakage and may best be provided by the surgeon's en-face view of the prosthetic MV from the left atrium (**Figure 11**). In addition, color 3D imaging may facilitate the differentiation of 3D drop-out artifacts from true defects.⁴¹⁾

CONCLUSION

Accurate description of the MR mechanism is crucial for determination of the need for and type of MV surgery. Addition of 3D echocardiography may be particularly helpful in identification of MV leaflet perforation, cleft, or prolapse and a more reproducible definition of MV annulus dilatation. The described modified classification by Shah and Raney provides a more comprehensive and detailed assessment of MV disorders. Further studies should investigate whether this modified classification has an impact on surgical techniques and outcome.

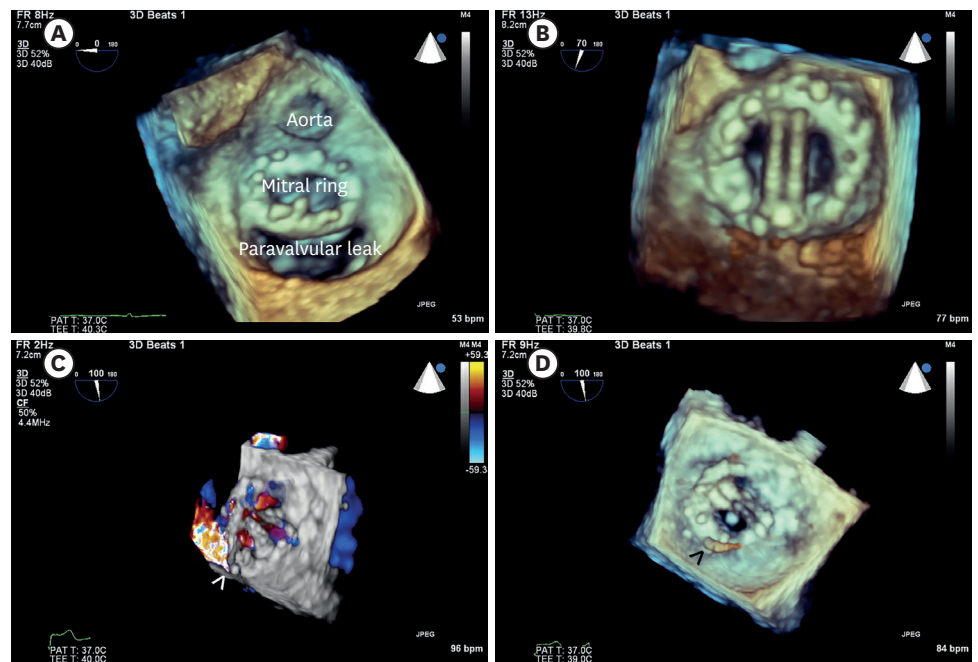


Figure 11. Three-dimensional echocardiography showing mitral ring dehiscence (A) and replacement with a mechanical prosthesis (B). The lower panel shows localization of smaller paravalvular leakage after implantation of a mechanical prosthesis by the origin of the 3D color Doppler jet (C, arrowhead), facilitating wire passage (D, arrowhead) and thus placement of a closure device.

REFERENCES

1. Surkova E, Muraru D, Aruta P, et al. Current clinical applications of three-dimensional echocardiography: When the technique makes the difference. *Curr Cardiol Rep* 2016;18:109.
[PUBMED](#) | [CROSSREF](#)
2. Lang RM, Badano LP, Tsang W, et al. EAE/ASE recommendations for image acquisition and display using three-dimensional echocardiography. *Eur Heart J Cardiovasc Imaging* 2012;13:1-46.
[PUBMED](#) | [CROSSREF](#)
3. McGhie JS, de Groot-de Laat L, Ren B, et al. Transthoracic two-dimensional xPlane and three-dimensional echocardiographic analysis of the site of mitral valve prolapse. *Int J Cardiovasc Imaging* 2015;31:1553-60.
[PUBMED](#) | [CROSSREF](#)
4. McGhie JS, Vletter WB, de Groot-de Laat LE, et al. Contributions of simultaneous multiplane echocardiographic imaging in daily clinical practice. *Echocardiography* 2014;31:245-54.
[PUBMED](#) | [CROSSREF](#)
5. Carpentier A. Cardiac valve surgery--the "French correction". *J Thorac Cardiovasc Surg* 1983;86:323-37.
[PUBMED](#)
6. de Groot-de Laat LE, Ren B, McGhie J, et al. The role of experience in echocardiographic identification of location and extent of mitral valve prolapse with 2D and 3D echocardiography. *Int J Cardiovasc Imaging* 2016;32:1171-7.
[PUBMED](#) | [CROSSREF](#)
7. Shah PM, Raney AA. New echocardiography-based classification of mitral valve pathology: relevance to surgical valve repair. *J Heart Valve Dis* 2012;21:37-40.
[PUBMED](#)
8. Shah PM, Raney AA. Echocardiography in mitral regurgitation with relevance to valve surgery. *J Am Soc Echocardiogr* 2011;24:1086-91.
[PUBMED](#) | [CROSSREF](#)
9. Ben Zekry S, Nagueh SF, Little SH, et al. Comparative accuracy of two- and three-dimensional transthoracic and transesophageal echocardiography in identifying mitral valve pathology in patients undergoing mitral valve repair: initial observations. *J Am Soc Echocardiogr* 2011;24:1079-85.
[PUBMED](#) | [CROSSREF](#)

10. Gutiérrez-Chico JL, Zamorano Gómez JL, Rodrigo-López JL, et al. Accuracy of real-time 3-dimensional echocardiography in the assessment of mitral prolapse. Is transesophageal echocardiography still mandatory? *Am Heart J* 2008;155:694-8.
[PUBMED](#) | [CROSSREF](#)
11. Beraud AS, Schnittger I, Miller DC, Liang DH. Multiplanar reconstruction of three-dimensional transthoracic echocardiography improves the presurgical assessment of mitral prolapse. *J Am Soc Echocardiogr* 2009;22:907-13.
[PUBMED](#) | [CROSSREF](#)
12. Dal-Bianco JP, Beaudoin J, Handschumacher MD, Levine RA. Basic mechanisms of mitral regurgitation. *Can J Cardiol* 2014;30:971-81.
[PUBMED](#) | [CROSSREF](#)
13. Thompson KA, Shiota T, Tolstrup K, Gurudevan SV, Siegel RJ. Utility of three-dimensional transesophageal echocardiography in the diagnosis of valvular perforations. *Am J Cardiol* 2011;107:100-2.
[PUBMED](#) | [CROSSREF](#)
14. Wyss CA, Enseleit F, van der Loo B, Grünenfelder J, Oechslin EN, Jenni R. Isolated cleft in the posterior mitral valve leaflet: a congenital form of mitral regurgitation. *Clin Cardiol* 2009;32:553-60.
[PUBMED](#) | [CROSSREF](#)
15. Looi JL, Lee AP, Wan S, et al. Diagnosis of cleft mitral valve using real-time 3-dimensional transesophageal echocardiography. *Int J Cardiol* 2013;168:1629-30.
[PUBMED](#) | [CROSSREF](#)
16. Guerreiro C, Fonseca C, Ribeiro J, Fontes-Carvalho R. Isolated cleft of the posterior mitral valve leaflet: the value of 3DTEE in the evaluation of mitral valve anatomy. *Echocardiography* 2016;33:1265-6.
[PUBMED](#) | [CROSSREF](#)
17. Lee AP, Jin CN, Fan Y, Wong RHL, Underwood MJ, Wan S. Functional implication of mitral annular disjunction in mitral valve prolapse: a quantitative dynamic 3D echocardiographic study. *JACC Cardiovasc Imaging* 2017;10:1424-33.
[PUBMED](#) | [CROSSREF](#)
18. Ennezat PV, Maréchaux S, Pibarot P, Le Jemtel TH. Secondary mitral regurgitation in heart failure with reduced or preserved left ventricular ejection fraction. *Cardiology* 2013;125:110-7.
[PUBMED](#) | [CROSSREF](#)
19. Oh JK, Seward JB, Tajik AJ. The Echo Manual. 3rd ed. Philadelphia: Lippincott Williams & Wilkins; 2006. p.211.
20. Galiuto L, Fox K, Sicari R, Zamorano JL, editors. The EAE Textbook of Echocardiography. Oxford: Oxford University Press; 2011. p.38-9.
21. Otto CM. Textbook of Clinical Echocardiography. 4th ed. Philadelphia: Saunders Elsevier; 2009. p.35-60.
22. Anwar AM, Soliman OI, Nemes A, et al. Assessment of mitral annulus size and function by real-time 3-dimensional echocardiography in cardiomyopathy: comparison with magnetic resonance imaging. *J Am Soc Echocardiogr* 2007;20:941-8.
[PUBMED](#) | [CROSSREF](#)
23. Foster GP, Dunn AK, Abraham S, Ahmadi N, Sarraf G. Accurate measurement of mitral annular dimensions by echocardiography: importance of correctly aligned imaging planes and anatomic landmarks. *J Am Soc Echocardiogr* 2009;22:458-63.
[PUBMED](#) | [CROSSREF](#)
24. Ren B, de Groot-de Laat LE, McGhie J, Vletter WB, Ten Cate FJ, Geleijnse ML. Geometric errors of the pulsed-wave Doppler flow method in quantifying degenerative mitral valve regurgitation: a three-dimensional echocardiography study. *J Am Soc Echocardiogr* 2013;26:261-9.
[PUBMED](#) | [CROSSREF](#)
25. Adams DH, Anyanwu AC. The cardiologist's role in increasing the rate of mitral valve repair in degenerative disease. *Curr Opin Cardiol* 2008;23:105-10.
[PUBMED](#) | [CROSSREF](#)
26. Adams DH, Anyanwu AC. Seeking a higher standard for degenerative mitral valve repair: begin with etiology. *J Thorac Cardiovasc Surg* 2008;136:551-6.
[PUBMED](#) | [CROSSREF](#)
27. Zamorano J, Cordeiro P, Sugeng L, et al. Real-time three-dimensional echocardiography for rheumatic mitral valve stenosis evaluation: an accurate and novel approach. *J Am Coll Cardiol* 2004;43:2091-6.
[PUBMED](#) | [CROSSREF](#)
28. Baumgartner H, Hung J, Bermejo J, et al. Echocardiographic assessment of valve stenosis: EAE/ASE recommendations for clinical practice. *Eur J Echocardiogr* 2009;10:1-25.
[PUBMED](#) | [CROSSREF](#)

29. Anwar AM, Attia WM, Nosir YF, et al. Validation of a new score for the assessment of mitral stenosis using real-time three-dimensional echocardiography. *J Am Soc Echocardiogr* 2010;23:13-22.
[PUBMED](#) | [CROSSREF](#)
30. Francis L, Finley A, Hessami W. Use of three-dimensional transesophageal echocardiography to evaluate mitral valve morphology for risk stratification prior to mitral valvuloplasty. *Echocardiography* 2017;34:303-5.
[PUBMED](#) | [CROSSREF](#)
31. Agricola E, Oppizzi M, Maisano F, et al. Echocardiographic classification of chronic ischemic mitral regurgitation caused by restricted motion according to tethering pattern. *Eur J Echocardiogr* 2004;5:326-34.
[PUBMED](#) | [CROSSREF](#)
32. Agricola E, Oppizzi M, Pisani M, Meris A, Maisano F, Margonato A. Ischemic mitral regurgitation: mechanisms and echocardiographic classification. *Eur J Echocardiogr* 2008;9:207-21.
[PUBMED](#)
33. Silbiger JJ. Mechanistic insights into ischemic mitral regurgitation: echocardiographic and surgical implications. *J Am Soc Echocardiogr* 2011;24:707-19.
[PUBMED](#) | [CROSSREF](#)
34. Levine RA, Schwammenthal E. Ischemic mitral regurgitation on the threshold of a solution: from paradoxes to unifying concepts. *Circulation* 2005;112:745-58.
[PUBMED](#) | [CROSSREF](#)
35. Veronesi F, Corsi C, Sugeng L, et al. Quantification of mitral apparatus dynamics in functional and ischemic mitral regurgitation using real-time 3-dimensional echocardiography. *J Am Soc Echocardiogr* 2008;21:347-54.
[PUBMED](#) | [CROSSREF](#)
36. Toida R, Watanabe N, Obase K, et al. Prognostic implication of three-dimensional mitral valve tenting geometry in dilated cardiomyopathy. *J Heart Valve Dis* 2015;24:577-85.
[PUBMED](#)
37. Bouma W, Lai EK, Levack MM, et al. Preoperative three-dimensional valve analysis predicts recurrent ischemic mitral regurgitation after mitral annuloplasty. *Ann Thorac Surg* 2016;101:567-75; discussion 575.
[PUBMED](#) | [CROSSREF](#)
38. Sherrid MV, Balaram S, Kim B, Axel L, Swistel DG. The mitral valve in obstructive hypertrophic cardiomyopathy: a test in context. *J Am Coll Cardiol* 2016;67:1846-58.
[PUBMED](#) | [CROSSREF](#)
39. Geleijnse ML, Krenning BJ, Nemes A, et al. Incidence, pathophysiology, and treatment of complications during dobutamine-atropine stress echocardiography. *Circulation* 2010;121:1756-67.
[PUBMED](#) | [CROSSREF](#)
40. Zamorano JL, Badano LP, Bruce C, et al. EAE/ASE recommendations for the use of echocardiography in new transcatheter interventions for valvular heart disease. *Eur Heart J* 2011;32:2189-214.
[PUBMED](#) | [CROSSREF](#)
41. Faletra FF, Ramamurthi A, Dequarti MC, Leo LA, Moccetti T, Pandian N. Artifacts in three-dimensional transesophageal echocardiography. *J Am Soc Echocardiogr* 2014;27:453-62.
[PUBMED](#) | [CROSSREF](#)